Measuring quantum correlations using lossy photon-number-resolving detectors with saturation

Si-Hui Tan[a*], Leonid A. Krivitsky[a] and Berthold-Georg Englert[b,c]

[a]*Data Storage Institute, Agency for Science, Technology and Research, 5 Engineering Drive 1, Singapore 117607, Singapore;* [b]*Centre for Quantum Technologies, National University of Singapore, 3 Science Drive 2, Singapore 117543, Singapore;* [c]*Department of Physics, National University of Singapore, 2 Science Drive 3, Singapore 117551, Singapore*

The variance of difference of photocounts is an established measure of quantum correlations for quantum states of light. It enables us to discriminate between the classical correlation of a two-mode coherent state and the quantum correlation of a twin-beam state. We study the effect of loss and saturation of the photon-number-resolving detector on the measurement of the variance of difference of photocounts. An analytic function is derived for this variance, both for the coherent and the twin-beam states. It is found that the variance of difference of photocounts is no longer a reliable entanglement measure in the non-linear regime of the detector response but it remains useful in some range of values of average photon numbers of the incident light. We also quantify the linear regime of the detector with saturation which will be useful for calibration of the detector quantum efficiency.

1. Introduction

Generation and characterization of multiphoton entangled states represent one of the prerogatives of modern quantum optics experiments. Highly-entangled multiphoton states such as NOON states [1] and photon-number-correlated twin-beam states [2] are promising resources for practical applications in quantum lithography [3], quantum metrology, [4] and quantum cryptography [5]. Measurement of the degree of quantum correlations accurately is an essential task for characterizing states of these types. The recent emergence of photon-number-resolving detectors (PNRDs) [6, 7], such as visible-light photon counters (VLPCs) [8], transition-edge sensors (TESs) [9], time-multiplexed detectors (TMDs) [10] and multipixel photon counters (MPPCs) [11], makes the direct characterization of multiphoton states by photocounting possible.

A measurement using a N-photon-resolving detector can be modeled by a positive-operator valued measure (POVM) with $N + 1$ outcomes: $\{\Pi_0, \Pi_1, \ldots, \Pi_N\}$, satisfying completeness, $\sum_{i=0}^{N} \Pi_i = I$, and positivity, $\Pi_i \geq 0, \forall\ i = 0, \ldots, N$. The outcomes of the POVM are diagonal in the Fock-state basis and hence phase insensitive. The probability of detecting i photons is $p_i' = \text{tr}(\rho \Pi_i)$, where the statistical operator ρ describes the photon state, and knowledge of the p_i's enables us to reconstruct the photon statistics. For a perfect detector with no loss (unit quantum efficiency) and no saturation, $\{\Pi_i = |i\rangle \langle i|, i = 1, 2, \ldots\}$. Then the probabilities p_i' should reflect the true frequency of occurrence of i photons received, p_i, in the limit of a large number of detection trials. However, because of loss and noise in the detector the measurement is a proper POVM rather than a von Neumann measurement and the measured probability p_i'

is a mixture of the actual photon statistics,

$$p'_i = \sum_j w_{ij} p_j \ , \tag{1}$$

where w_{ij} is the conditional probability of detecting i photons when j photons impinged on the detector. The conditional probabilities model the measurement process in the detector; in the POVM picture, they are related to the outcomes by $w_{ij} = \langle j | \Pi_i | j \rangle$, where $|j\rangle$ is the ket of the Fock state with j photons. The set of w_{ij} has been used to quantify the capability of photon number discrimination of the PNRD [12], and the objective of detector tomography is to determine the conditional probabilities w_{ij} in a model-free way [13–15]. However, detector tomography relies on the ability to prepare a tomographically complete set of states and complicated optimization techniques. Therefore, parameter estimation for instrument calibration requires suitable models for the POVM [11, 16–20].

Highly entangled states can be produced in various nonlinear optical processes [21]. At high intensities, the photodetector response becomes nonlinear due to saturation. For example, in a silicon multi-pixel photodetector consisting of a spatial array of avalanche photodiodes (APD), saturation of individual APDs in the silicon multi-pixel detector results in the saturation of the array. TES is another alternative for PNRD, which exploits bolometric methods for photon detection. TESs operate at cryogenic temperatures (below 100mK) and have high quantum efficiency ($\sim 95\%$). Their saturation at high intensities is due to the heating of the detectors beyond the superconducting state. Hence, there is a clear need to understand the effects of saturation so that one can use these PNRDs in experiments with intense non-classical states of light.

In this paper, we assess the feasibility of using lossy PNRDs for measuring quantum correlations under joint photodetection in the presence of saturation. The figure of merit that we use here is the variance of difference of photocounts (VDP), which has been shown to be a good measure of entanglement [22]. The dependence of the VDP on quantum efficiencies of photodetectors has been exploited in the method of absolute calibration of quantum efficiency using twin-beam light [23–25]. The effects of saturation on this calibration protocol will be discussed here too.

This paper is organized as follows: In Section 2, the joint detection setup is described. The POVM modeling of losses and saturation are presented. The first and second moments of the photocounts of these POVM for a state with Poissonian statistics are derived. In Section 3, the VDP and its moment operators are described. The VDP of two pairs of two-mode states, one with classical and another with quantum correlations, are calculated. The difference of these VDP, Q, is introduced as a measure of distinguishability between quantum and classical correlations. A tractable analytic form is derived for Q. In Section 4, we introduce the noise reduction factor (NRF), a normalized form of the VDP, and show how an absolute calibration of two detectors can be performed using the NRF in the linear regime of the detector response. The analytic form of the photocount calculated in Section 2 gives a quantitative estimate for the range of mean photon numbers in which the detector remains linear. In Section 5, the results are summarized and the use and limitations of the measurement model are discussed.

2.   Modeling photon detection with loss and saturation

The joint measurement scheme is as follows: Two modes of radiation with the mode creation operators, a_1 and a_2, are incident on two PNRDs. The resulting photocounts of the respective PNRDs are analyzed. The joint detection of quantum correlations with lossy photodetectors has been looked into in [22]. Here we extend the theory to include the effects of saturation. For the

purpose of the analysis, we use the twin-beam (TWB) state defined as

$$|X\rangle = \sum_{n=0}^{\infty} b_n |n\rangle_1 |n\rangle_2 \ , \tag{2}$$

where $|n\rangle_j$, $j = 1, 2$ is the Fock state with n photons in mode j and b_n is the probability amplitude of the state $|X\rangle$. It follows from the structure of Eqn. (2) that the two modes of the TWB state are perfectly correlated in photon numbers. The TWB state can be generated by spontaneous parametric downconversion (SPDC) in a nonlinear crystal pumped by a pulsed laser. The two beams created by SPDC comprise inherently of multiple frequency modes. In the limit of a large number of these modes, $|b_n|^2 = \exp(-\bar{n})\bar{n}^n/n!$, where $\bar{n}$ is the mean number of photons in either the signal or the idler mode [26, 27]. As a standard for comparison with classical states, we shall use the two-mode coherent (TMC) state $|\alpha\rangle_1 |\alpha\rangle_2$ where $\bar{n} = |\alpha|^2$. Without loss of generality, we can assume that there is no phase difference between the two modes in the TMC state because photocounting is a phase-insensitive measurement.

The mth outcome of the POVM of a lossy detector with quantum efficiency η is given by [28],

$$\Pi_m = \sum_{n=m}^{\infty} w_{m,n}(\eta)|n\rangle\langle n| \ , \tag{3}$$

with

$$w_{m,n}(\eta) = \eta^m (1 - \eta)^{n-m} \binom{n}{m} \ , \tag{4}$$

for $m = 0, 1, 2 \ldots$ and $w_{m,n}(\eta)$ was introduced in Eqn. (1). For a PNRD, the measured number of photons, m, which is an eigenvalue of the photocount, $\widehat{m}$, has an upper bound at N. When $m < N$, then its POVM is the same as in Eqn. (3), but because the PNRD is unable to resolve between N and $N + 1$ or more photons, we have

$$\Pi_N = I - \sum_{m=0}^{N-1} \Pi_m \ , \tag{5}$$

for the Nth outcome. N is the maximum resolvable photocount. When N or more photons are incident on the detector, at most N photons will be registered. When $N = 1$, this POVM reduces to that of the ON/OFF photodetector: $\{\Pi_0, \Pi_1\}$, where $\Pi_0 = \sum_{n=0}^{\infty}(1 - \eta)^n |n\rangle\langle n|$ and $\Pi_1 = I - \Pi_0$.

Given the outcomes of a joint measurement of a two-mode state ρ, the joint probability distribution is given by $p(m_1, m_2) = \text{tr}(\rho\Pi_{m_1} \otimes \Pi_{m_2})$. Moments of this distribution, $\langle \widehat{m_1^p}\widehat{m_2^q} \rangle$ can be calculated via the p-moment operator of the photocount,

$$\widehat{m^p} = \sum_{m=0}^{N-1} m^p \Pi_m$$

$$= N^p I - \sum_{m=0}^{N-1} \sum_{n=m}^{\infty} (N^p - m^p) B_{m,n}(\eta)|n\rangle\langle n| \ . \tag{6}$$

We note that since they are the operatorial moments of a POVM, $\widehat{m^p} \neq \widehat{m}^p$ [22] unless the outcomes Π_m are pairwise orthogonal which is not the case here. The first two moment operators

are

$$\widehat{m} = \eta\widehat{n} - \sum_{n=N+1}^{\infty} C_n(N,\eta)\,|n\rangle\,\langle n|\ ,\tag{7}$$

and

$$\widehat{m^2} = \eta^2\,\widehat{n}^2 + \eta(1-\eta)\widehat{n} - (2N+1)\sum_{n=N+1}^{\infty} C_n(N,\eta)|n\rangle\langle n| + 2\sum_{n=N+2}^{\infty} D_n(N,\eta)|n\rangle\langle n|\ ,\tag{8}$$

where

$$C_n(N,\eta) \equiv \binom{n}{N+1} x^{N+1}(1-\eta)^n F(2, N-n+1, N+2|-x)\ ,$$

$$D_n(N,\eta) \equiv \binom{n}{N+2} x^{N+2}(1-\eta)^n F(3, N-n+2, N+3|-x)\ ,\tag{9}$$

with $x = \eta/(1-\eta)$ and $F(a,b,c|x)$ is Gauss's hypergeometric function.

Without saturation, the first and second moment operators are $\widehat{m}_0 = \eta\widehat{n}$ and $\widehat{m_0^2} = \eta^2\widehat{n}^2 + \eta(1-\eta)\widehat{n}$ respectively. The variance of the photocounts is then $\sigma^2(m) = \langle\widehat{m^2}\rangle - \langle\widehat{m}\rangle^2 = \eta^2\sigma^2(n) + \eta(1-\eta)\,\langle\widehat{n}\rangle$. It is clear from Eqs. (7)-(9) that the saturation adds extra summation terms into the moment operators. For a state with Poissonian statistics we have

$$\langle\widehat{m}\rangle_{\mathrm{P}} = N - [Ne_{N-1}(\eta\bar{n}) - \eta\bar{n}e_{N-2}(\eta\bar{n})]e^{-\eta\bar{n}}\ ,$$

$$\langle\widehat{m^2}\rangle_{\mathrm{P}} = N^2 - \frac{(\eta\bar{n})^N(N+\eta\bar{n})e^{-\eta\bar{n}}}{\Gamma(N)} + [(\eta\bar{n})^2 + \eta\bar{n} - N^2]e^{-\eta\bar{n}}e_{N-1}(\eta\bar{n})\ ,\tag{10}$$

where $e_n(x)$ is the exponential sum function

$$e_n(x) = \sum_{k=0}^{n} \frac{x^k}{k!}\ .\tag{11}$$

The dependence of the average photocount of a single detector on the average photon number of an impinging Poissonian light is shown in Figure 1. When $\bar{n} \to \infty$, the average number of photocounts tends to the saturation value N with the following behavior:

$$\langle\widehat{m}\rangle_{\mathrm{p}} = N + \mathcal{O}\left(\frac{1}{\bar{n}^2}\right) - e^{-\eta\bar{n}}\bar{n}^N\left(\frac{\eta^{N-1}}{(N-1)!\bar{n}} - \mathcal{O}\left(\frac{1}{\bar{n}^2}\right)\right)\ .\tag{12}$$

By contrast when $\bar{n} \ll N$, the saturation effect is negligible so the expected detected photons behave like that without saturation,

$$\langle\widehat{m}\rangle_{\mathrm{p}} = \eta\bar{n} + \mathcal{O}\left(\bar{n}^2\right) - \bar{n}^N\left(\frac{\eta^{1+N}\bar{n}}{(N+1)!} - \mathcal{O}(\bar{n}^2)\right)\ .\tag{13}$$

When $(\eta\bar{n})^N \ll (N+1)!$, then $\langle\widehat{m}\rangle_{\mathrm{P}} = \eta\bar{n}$ which identifies the linear regime of the detector. The POVM in Eqs. (3)-(5) describes the average photocount of a detector expected in the asymptotic limit of small and large average impinging photon number.
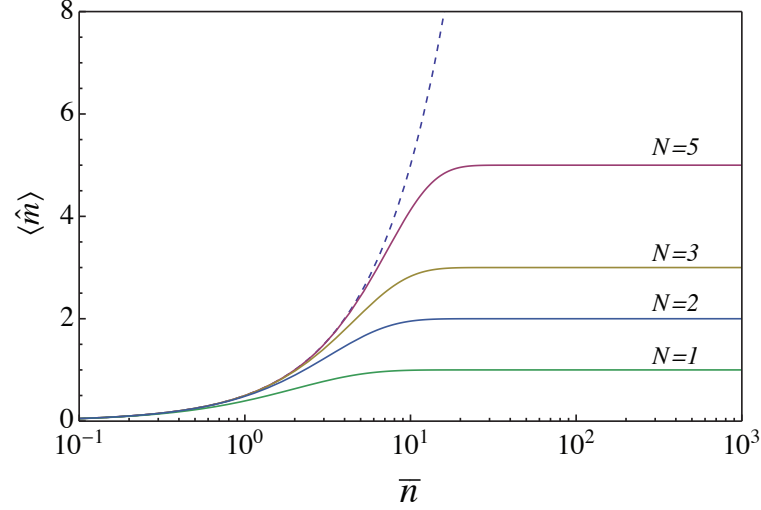
Figure 1. A plot of the detected photocount $\langle \widehat{m} \rangle$ with the average number of photons $\bar{n}$ in the incident beam for the lossy detector with various maximum photocount of the detector, N (solid), and quantum efficiency, $\eta = 0.5$. Quantum efficiency which is defined to be the ratio of the detected photocount to the incident photon number, i.e. the slope of the detected photon curve, tends to 0 at large $\bar{n}$. The response of a detector with just loss is also shown (dotted) for comparison.

3. Variance of Difference

Given the two photocounts from the joint detection, their difference is

$$\widehat{D} = \widehat{m}_1 - \widehat{m}_2 \ , \tag{14}$$

with integer eigenvalues $d = 0, \pm 1, \pm 2, \dots$. The POVM of the measurement of the difference photocount, Θ_d, is

$$\Theta_d = \sum_{q=0}^{N-|d|} \begin{cases} \Pi_{q+d} \otimes \Pi_q & , \ d > 0 \\ \Pi_q \otimes \Pi_q & , \ d = 0 \\ \Pi_q \otimes \Pi_{q-d} & , \ d < 0 \end{cases} , \tag{15}$$

where Π_m is the mth POVM outcome of Eqn. (3). The moments of the difference photocount distribution are then

$$\widehat{D} = \sum_d d\Theta_d = \widehat{m}_1 - \widehat{m}_2 \ ,$$

$$\widehat{D^2} = \sum_d d^2 \Theta_d = \widehat{m_1^2} + \widehat{m_2^2} - 2\widehat{m}_1 \widehat{m}_2 \ . \tag{16}$$

The VDP for a given quantum state is $\sigma^2(d) = \langle \widehat{D^2} \rangle - \langle \widehat{D} \rangle^2$. Let us find the VDP for the TMC and the TWB states. For the TMC state, we get

$$\sigma_\alpha^2(d) = \sigma_\alpha^2(m_1) + \sigma_\alpha^2(m_2) \ , \tag{17}$$

where $\sigma_\alpha^2(m_j) = \langle \widehat{m_j^2} \rangle_{\rm p} - \langle \widehat{m_j} \rangle_{\rm p}^2$. For the TWB state, the quantum correlations gives nonzero terms in the covariance of the joint photostatistics and this shows up in the VDP,

$$\sigma_X^2(d) = \sigma_\alpha^2(m_1) + \sigma_\alpha^2(m_2) - 2\langle \widehat{m}_1 \widehat{m}_2 \rangle_X + 2\langle \widehat{m}_1 \rangle_{\rm p} \langle \widehat{m}_2 \rangle_{\rm p} \ , \tag{18}$$

where

$$\langle \widehat{m}_1 \widehat{m}_2 \rangle_X = \eta_1 \eta_2 \bar{n}(1 + \bar{n}) - \sum_{n=N_2}^{\infty} |b_n|^2 \eta_1 n C_n(N_2, \eta_2) - \sum_{n=N_1}^{\infty} |b_n|^2 \eta_2 n C_n(N_1, \eta_1)$$

$$+ \sum_{n=\max(N_1,N_2)}^{\infty} |b_n|^2 C_n(N_1, \eta_1) C_n(N_2, \eta_2) \ . \tag{19}$$

In Figure 2, we show the effects of loss and saturation on measuring the VDP for the TMC and the TWB states with different values of $N_1 = N_2 = N$ and $\eta_1 = \eta_2 = \eta$. Two observations can be made. First, the saturation causes the variance to decrease with increasing average photon number for both the TMC and the TWB states and asymptotically approach zero. This means that the VDP cannot provide a reliable discrimination of classical and quantum correlations at values of $\bar{n}$ that are too large. Second, loss degrades the measurement of the quantum correlation since with increasing loss, the VDP for the TWB becomes closer to that for the TMC.

However, there exists a range of $\bar{n}$ for such a discrimination to be possible. Let us define a quantity Q by means of

$$Q \equiv Q(N_1, N_2, \eta_1, \eta_2, \bar{n}) = \sigma_\alpha^2(d) - \sigma_X^2(d) \ . \tag{20}$$

Q is an indication of how good the discrimination between the classical and quantum correlations is. Figure 3 shows the behavior of Q versus $\bar{n}$ for the TMC and TWB states. The optimal discrimination happens for the largest Q values for some $\bar{n}_{\max}$ that we can solve for if we know the quantum efficiencies, η, and the maximum photocount of the detector, N, of the detectors. The optimal discrimination does not always occur when $\eta = 1$ due to saturation. When the mean photon number is high and saturation is likely to occur, having some loss in the detectors will help to set off the effect of saturation. However, loss will degrade the quality of the measurement of the VDP. As such, there is an interplay between loss and saturation.

The analytic forms for the VDP for the TMC and TWB states measured by a PNRD with saturation and loss in Eqs. (17)-(19) are the main results of the paper. Using these results, we analyzed the VDP for different values of η and N thus illustrating the significance of loss and saturation to the measurement of the VDP. Thus, such an analytic analysis is helpful for interpreting experimental data. We will also show in the next section, how we can use the features of saturation in the analytic model in the absolute calibration of the PNRDs.

4.   Absolute Calibration of PRNDs using the NRF

Sometimes it is helpful to consider a related measure of quantum correlation— the noise reduction factor (NRF),

$$\mathrm{NRF} = \frac{\sigma^2(d)}{\langle \widehat{m}_1 \rangle + \langle \widehat{m}_2 \rangle} \ . \tag{21}$$
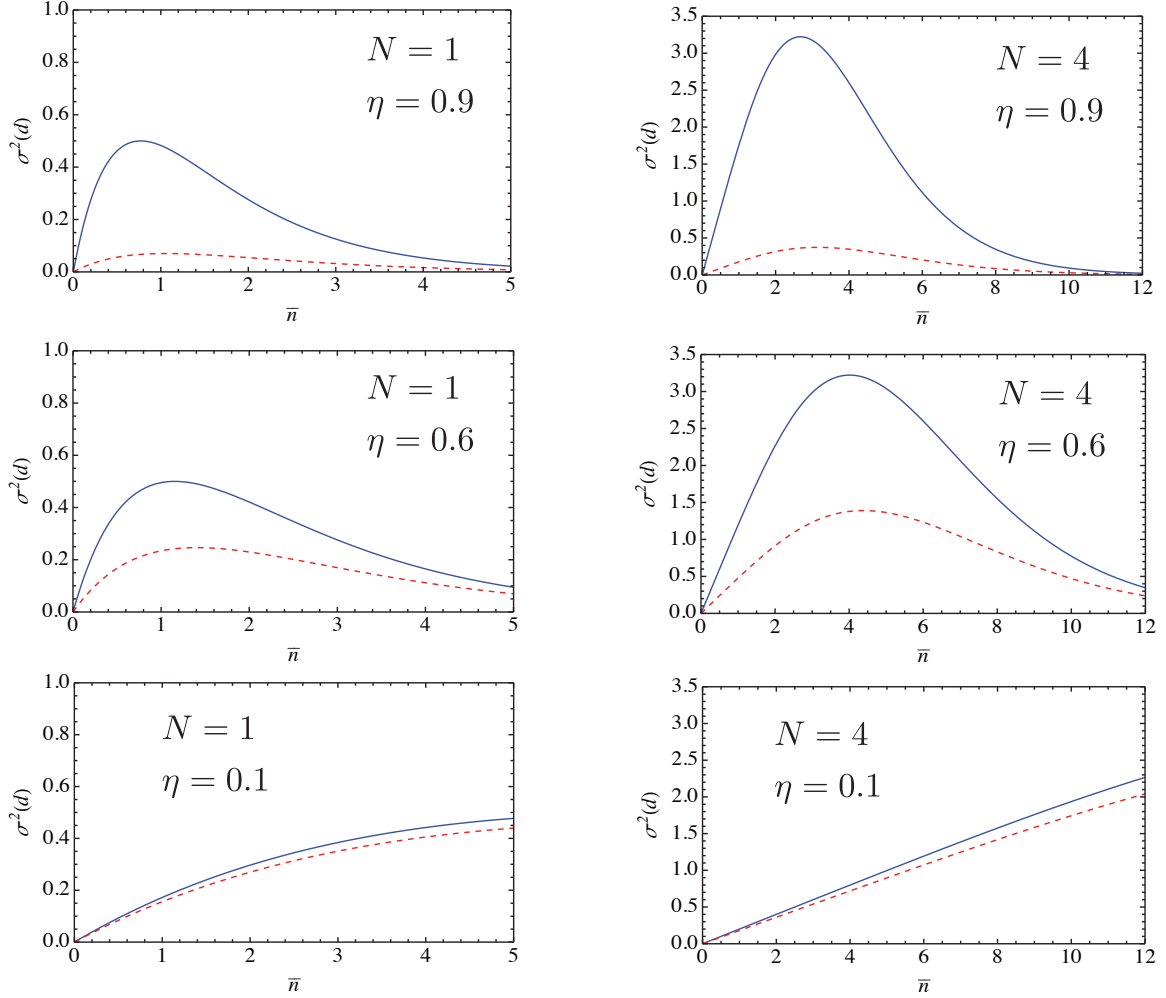
Figure 2. (Color online) Variance of the difference of photocounts (VDP), $\sigma^2(d)$, as a function of the mean photon number of the input signal for the TMC state (blue solid line) and the TWB state (red dashed line), where $\eta_1 = \eta_2 = \eta$ and $N_1 = N_2 = N$ with various values of N and η to illustrate the effects of saturation and loss.

For the TMC state, NRF $= 1$ with any value of quantum efficiencies for the detectors. For the TWB, NRF $= 0$ with detectors of perfect quantum efficiencies and NRF $= 1 - \frac{2\eta_1\eta_2}{\eta_1+\eta_2}$ with lossy detectors, where η_1 and η_2 are their respective quantum efficiencies. This makes the NRF a useful measure of quantum correlations for two-mode states, as well as a calibration measure for the quantum efficiencies of detectors [25]. First, we will describe the current experimental procedure for absolute calibration which is possible in the linear regime of a PNRD. Then using the analytic form for the photocount, a range of values of average photon number for the linear regime can be derived. Second, we will suggest the use of the analytic form in Eqn. (17)-(19) for absolute calibration beyond the linear regime of the PNRD.

For the first method, let us consider the scenario in which we are given two detectors with unknown quantum efficiencies and saturation characteristics. Absolute calibration, for example, can be achieved if we have a TWB state by measuring NRF in the linear regime of the detectors. The calibration routine is as follows:

(1) Measure the photocounts, $\langle \widehat{m}_1 \rangle$ and $\langle \widehat{m}_2 \rangle$, of the two detectors with increasing $\bar{n}$. This can be done by increasing the pump power of the laser. From this data, the mean photocounts, VDP, and consequently the NRF, can be calculated.

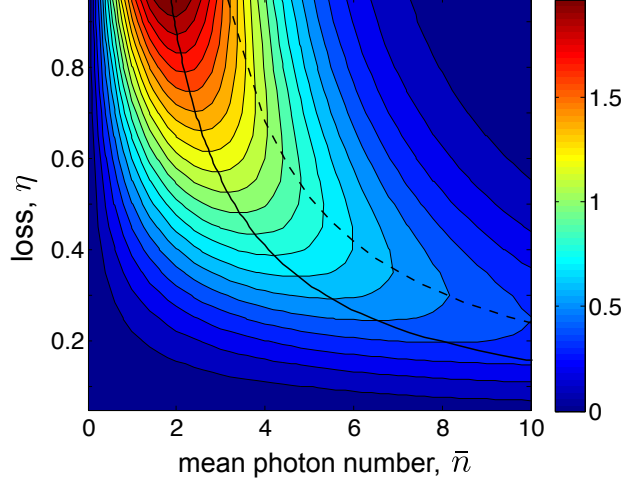(2) Let us define the ratio of the two quantum efficiencies, $k = \frac{\eta_1}{\eta_2}$. In the regime where the

Figure 3. (Color online) A contour plot of Q versus mean photon number, $\bar{n}$, and loss, η, for a balanced joint detection where $\eta_1 = \eta_2 = \eta$ and $N_1 = N_2 = 3$. In this figure, the maximum Q value is clearly visible. The solid line shows the optimal $\bar{n}$ for a given η and the dashed line shows the optimal η for a given $\bar{n}$. The higher the value of Q, the better the discrimination between quantum and classical correlations. Note that for a fixed value of $\bar{n}$, the best discrimination does not always occur at $\eta = 1$ (zero loss). A higher loss is favored at higher mean photon numbers where saturation gets more prevalent to obtain a larger Q value. However, higher losses in the photocount will degrade the measurement of the VDP.

photocounts are approximately linear with respect to $\bar{n}$, then, $\frac{\langle \widehat{m}_1 \rangle}{\langle \widehat{m}_2 \rangle} \approx k$. So k can be found by calculating the ratios of the two photocounts.

(3) For this range of average photon number, $\text{NRF} = 1 - \frac{2\eta_1}{1+k}$. Using the measured NRF and the value of k found in Step (2) above, η_1 can be calculated. Last, we can calculate η_2 from the values of k and η_1 found.

Thus, absolute calibration of the detector is possible in the linear regime of the detector. This is quantified by the range of $\bar{n}$ in which the term linear in $\bar{n}$ is much larger than the next order term in Eqn. (10),

$$\frac{(\eta\bar{n})^N}{(N+1)!} \ll 1 . \tag{22}$$

The higher the saturation point is, the broader the linear regime of the detector. Although it is difficult to pinpoint exactly how small the value on the left-hand side of Eqn. (22) must be, current experiments suggest that values of ~ 0.1 are sufficient [6]. The worst range of values of $\bar{n}$ for the linear regime is given for $N = 1$, where we would require that $\bar{n} < \frac{0.1}{\eta}$. For an APD where $N = 1$, the quantum efficiency is typically of order 33% [19], thus the linear regime is where $\bar{n} < 0.6$. However, for a VLPC with a typical saturation value of $N = 10$ and quantum efficiency $\eta = 85\%$ [19], we have $\bar{n} < 5.4$. So the linear regime of the VLPC is about 9 times that of the APD. This puts a quantitative estimate for the linear regime of a PNRD from its characteristics which are typical for that type of detector and can be taken from its manual. Once an approximate linear regime is determined, a careful calibration can be done in this range of average photon numbers.

In principle, using the analytic forms in Eqs. (10), (17) and (19), we can achieve absolute calibration beyond the linear regime of the PNRD with just a TMC state using the following protocol:

(1) Split a pulsed laser beam with a 50-50 non-polarizing beamsplitter into two parts with equal intensities to form a TMC state. One has to make sure that the laser produces a

(2) Measure the photocounts of the beam in each arm with a detector where the detection intervals are triggered by the laser. Then increase $\bar{n}$ by increasing the pump power until there is no visible change in the mean photocount with increasing $\bar{n}$. In this limit, the detectors are saturated and we have $N_1 = [\langle \widehat{m}_1 \rangle_{\text{sat}}]$ and $N_2 = [\langle \widehat{m}_2 \rangle_{\text{sat}}]$, where the subscript "sat" indicates values at saturation and $[\cdot]$ denotes the closest integer.

(3) Calculate the difference of photocounts for each detection interval and then the variance of this difference for each $\bar{n}$ value.

(4) Using the found values of N_1 and N_2 we can generate an equation for the NRF of the TMC state as measured by the PNRD from Eqs. (1), (17) and (19). A nonlinear fit of the experimental data of the VDP for the TMC state can then be done with the analytic form for the NRF using a suitable numerical algorithm. This will yield fitted values of η_1 and η_2 thus completing the calibration of the PNRDs.

This absolute calibration procedure with the TMC state is possible owing to the features of the VDP in the presence of saturation. It would not be possible if detectors operating in the linear regime or detectors with just losses are used, because in those cases, the VDP would be insensitive to the quantum efficiencies of the detectors. The advantage of using this second method instead of the first is that we do not have to rely on a TWB state which are harder to generate than a TMC state. The disadvantage is that we have to use a numerical nonlinear fit method for the calibration which might yield more than one reasonable fit and the errors in these fittings are generally larger than those for a linear regression fit required for the first method.

5.   Conclusion

A model of joint photodetection with lossy detectors considering saturation is presented. Using this model, we have derived an analytic form for the VDP which is tractable for calculations. We then used this analytic form to study the effects of saturation on measurements of the VDP. It has been found that saturation diminishes this measure and the variance of photocounts of the TMC and TWB states cannot be distinguished at large mean photon numbers. Loss in the PNRDs degrades the quality of the measurement of the quantum correlation. On the other hand, loss can offset the effects of saturation at high average photon numbers. Nonetheless, the VDP is still a good measure of quantum correlations as long as we are not far from the optimal Q.

Saturation also limits the range of $\bar{n}$ in which data is useful for calibration. This has been known for some time experimentally, but here we have derived quantitatively what this range is in terms of relative values of quantum efficiency and saturation value. With the analytic forms for the measured photocounts and VDP, we will also be able to do an absolute calibration with a TMC state. The generation of a TMC state is far simpler than that of a TWB state where the latter is required for absolute calibration.

As the focus of this paper is on loss and saturation effects in PNRDs, we have not looked at possible extensions of the measurement model. For example, apart from loss and saturation, PNRDs can also suffer from dark counts and crosstalk effects, both of which add spurious counts to the data. In using the measurement model for accounting for noise in actual experiments, one would have to take these effects into account. This can be done by modifying Eqn. (3) with the appropriate conditional probability matrices representing different noise types. Another useful extension of the measurement model is that of a variable saturation value, N. Here, we have considered a fixed saturation value but in practice, a PNRD can have different saturation values at different intensities or wavelengths of incident light. A more robust measurement model can be obtained by taking this variability into account.

Acknowledgement

References

[1] Afek, I.; Ambar, O.; Silberberg, Y. High-NOON states by mixing quantum and classical light. *Science* **2010**, *328*, 879.

[2] Bondani, M.; Allevi, A.; Zambra, G.; Paris, M.G.A.; et al. Sub-shot-noise photon-number correlation in a mesoscopic twin beam of light. *Phys. Rev. A* **2007**, *76*, 013833.

[3] Boto, A.N.; Kok, P.; Abrams, D.S.; Braunstein, S.L.; Williams, C.P.; et al. Quantum Interferometric Optical Lithography: Exploiting Entanglement to Beat the Diffraction Limit. *Phys. Rev. Lett.* **2000**, *85*, 2733–2736.

[4] Giovannetti, V.; Lloyd, S.; Maccone, L. Quantum Metrology. *Phys. Rev. Lett.* **2006**, *96*, 010401.

[5] Ekert, A.K. Quantum Cryptography based on Bell's Theorem. *Phys. Rev. Lett.* **1991**, *67*, 661–663.

[6] Eisaman, M.D.; Fan, J.; Migdall, A.; et al. Single-photon sources and detection. *Rev. Sci. Instrum.* **2011**, *82*, 071101.

[7] Hadfield, R.H. Single-photon detectors for optical quantum information applications. *Nature Photonics* **2009**, *3*, 696–705.

[8] Kim, J.; Takeuchi, S.; Yamamoto, Y.; et al. Multiphoton detection using visible light photon counter. *Appl. Phys. Lett.* **1999**, *74*, 902–904.

[9] Rosenberg, D.; Lita, A.E.; Miller, A.J.; et al. Noise-free high-efficiency photon-number-resolving detectors. *Phys. Rev. A* **2005**, *71*, 061803(R).

[10] Fitch, M.J.; Jacobs, B.C.; Pittman, T.B.; et al. Photon-Number Resolution using Time-Multiplexed Single-photon detectors. *Phys. Rev. A* **2003**, *68*, 043814.

[11] Afek, I.; Natan, A.; Ambar, O.; et al. Quantum State measurements using multipixel photon detectors. *Phys. Rev. A* **2009**, *79*, 043830.

[12] Lee, H.; Yurtsever, U.; Kok, P.; Hockney, G.M.; Adami, C.; Braunstein, S.L.; et al. Towards photostatistics from photon-number discriminating detectors. *J. Mod. Opt* **2004**, *51*, 1517–1528.

[13] Feito, A.; Lundeen, J.S.; Coldenstrodt-Ronge, H.; Eisert, J.; Plenio, M.B.; et al. Measuring Measurement: Theory and Practice. *N. J. Phys.* **2009**, *11*, 093038.

[14] Lundeen, J.S.; Feito, A.; Coldenstrodt-Ronge, H.; Pregnell, K.L.; Silberhorn, Ch.; Ralph, T.C.; Eisert, J.; Plenio, M.B.; et al. Tomography of Quantum Detectors. *Nature Phys.* **2009**, *5*, 27–30.

[15] D'Ariano, G.M.; Maccone, L.; Presti, P.L. Quantum Calibration of Measurement Instrumentation. *Phys. Rev. Lett.* **2004**, *93*, 250407.

[16] Ramilli, M.; Allevi, A.; Chmill, V.; Bondani, M.; Caccia, M.; et al. Photon-number Statistics with Silicon Photomultipliers. *J. Opt. Soc. Am. B* **2010**, *27* (5), 852–862.

[17] Kalashnikov, D.A.; Tan, S.H.; Chekova, M.V.; et al. Accessing Photon Bunching with a Photon Number Resolving multi-pixel detector. *Opt. Express* **2011**, *19* (10), 9352–9363.

[18] Eraerds, P.; Legré, M.; Rochas, A.; Zbinden, H.; et al. SiPM for fast photon-counting and multiphoton detection. *Opt. Express* **2007**, *15* (22), 14539–14549.

[19] Kok, P.; Lovett, B.W. Introduction to Optical Quantum Information Processing. Cambridge University Press: Cambridge, UK, 2010.

[20] Sperling, J.; Vogel, W.; Agarwal, G.S. True photocounting statistics of multiple on-off detectors. *Phys. Rev. A* **2012**, *85*, 023820.

[21] Glöckl, O.; Anderson, U.L.; Leuchs, G. Verifying continuous-variable entanglement of intense light pulses. *Phy. Rev. A* **2006**, *73*, 012306.

[22] Agliati, A.; Bondani, M.; Andreoni, A.; deCillis, G.; et al. Quantum and Classical Correlations of Intense beams of light investigated via Joint Photodetection. *J. Opt. B: Quantum Semiclass. Opt.* **2005**, *7*, S652–S663.

[23] Klyshko, D.N. Use of two-photon light for absolute calibration of photoelectric detectors. *Sov. J. Quantum Electron* **1980**, *7* (9), 1112–1116.

[24] Brida, G.; Genovese, M.; Gramegna, M. Twin-photon techniques for photo-detector calibration. *Laser Phys. Lett.* **2006**, *3*, 115–123.

[25] Agafonov, I.N.; M.V.Chekhova; Iskhakov, T.S.; Penin, A.N.; et al. Absolute calibration of photodetectors: photocurrent multiplication versus photocurrent subtraction. *Opt. Lett.* **2011**, *36*, 1329-1331.

[26] Waks, E.; Sanders, B.C.; Diamanti, E.; et al. Highly nonclassical photon statistics in parametric down-conversion. *Phys. Rev. A* **2006**, *73*, 033814.

[27] Haderka, O.; Peřina, J., Jr.; M.Hamar; et al. Direct measurement and reconstruction of nonclassical features of twin beams generated in spontaneous parametric down-conversion. *Phys. Rev. A* **2005**, *71*, 033815.

[28] Ferraro, A.; Olivares, S.; Paris, M.G.A. Gaussian states in continuous variable quantum information. *Preprint* **2005**, *quant-ph/0503237v1*.

[29] Bachor, H.; Ralph, T.C. A Guide to Experiments in Quantum Optics.2nd; Wiley-VCH: Weinheim, Germany, 2004.